

Temperature dependence of the dielectric function and interband critical points in silicon

P. Lautenschlager, M. Garriga, L. Viña,* and M. Cardona

Max-Planck-Institut für Festkörperforschung, Heisenbergstrasse 1, D-7000 Stuttgart 80, Federal Republic of Germany

(Received 30 April 1987)

The complex dielectric function $\epsilon(\omega)$ of Si was measured ellipsometrically in the 1.7–5.7-eV photon-energy range at temperatures between 30 and 820 K. The observed structures are analyzed by fitting the second-derivative spectrum $d^2\epsilon/d\omega^2$ with analytic critical-point line shapes. Results for the temperature dependence of the parameters of these critical points, labeled E'_0 , E_1 , E_2 , and E'_1 , are presented. The data show good agreement with microscopic calculations for the energy shift and the broadening of interband transitions with temperature based on the electron-phonon interaction. The character of the E_1 transitions in semiconductors is analyzed. We find that for Si and light III-V or II-VI compounds an excitonic line shape represents best the experimental data, whereas for Ge, α -Sn, and heavy III-V or II-VI compounds a two-dimensional critical point yields the best representation.

I. INTRODUCTION

The macroscopic linear optical response of Si is represented by the dielectric function $\epsilon(\omega)$ which is closely related to the electronic band structure of the material. The structures observed in the $\epsilon(\omega)$ spectra are attributed to interband transitions (critical points) which can be analyzed in terms of standard analytic line shapes:^{1,2}

$$\epsilon(\omega) = C - Ae^{i\Phi}(\omega - E + i\Gamma)^n, \quad (1)$$

where a critical point (CP) is described by the amplitude A , threshold energy E , broadening Γ , and the excitonic phase angle Φ . The exponent n has the value $-\frac{1}{2}$ for one-dimensional (1D), 0 [logarithmic, i.e., $\ln(\omega - E + i\Gamma)$] for 2D, and $\frac{1}{2}$ for 3D CP's. Discrete excitons are represented by $n = -1$. The information obtained from the line-shape analysis can be compared with band-structure calculations.

The band structure of Si calculated by the $\mathbf{k}\cdot\mathbf{p}$ method,³ including the location of several direct interband transitions related to CP's at different parts of the Brillouin zone (BZ), is shown in Fig. 1. The lowest absorption edge of Si corresponds to indirect transitions from the highest valence band at the Γ point to the lowest conduction band near X . The lowest direct energy gap, labeled E'_0 and located at the Γ point, is nearly degenerated with the E_1 transitions, which take place along the Λ directions of the BZ. The next higher transitions are called E_2 , sometimes assigned to the X points which, however, participate only weakly in them, and E'_1 , also along the Λ line, but involving the second lowest conduction bands. Measurements of these direct interband transitions have been performed by several optical techniques, such as reflectance^{4,5} and ellipsometry^{6,7} as well as several reflectance-modulation techniques such as magnetorefectance,⁸ thermorefectance,^{9,10} electroreflectance,¹¹⁻¹⁸ and wavelength-modulated reflectance.^{19,20} The temperature dependence of the E_1 and E_2 CP's up to 300 K has been investigated by reflectance,⁵ wavelength-modulated reflectance,¹⁹ thermorefectance,¹⁶ and piezoreflectance.²¹ The temper-

ature coefficient of the energy of the E_1 CP has been determined by resonant Raman scattering.²² The shift of the E'_0 and E_2 transitions has been obtained from the maxima in the dielectric function in the 10–972-K temperature range.⁷ Many band-structure calculations have been performed with various semiempirical methods.²³⁻²⁵ In addition, the effect of spin-orbit splitting on the band structure has been studied in some detail.²⁶⁻²⁸

For calculations of the temperature dependence of CP energies, both the effect of thermal expansion and electron-phonon interaction has to be taken into account. In earlier works, the latter effect was included by softening the pseudopotential form factors with temperature-dependent Debye-Waller factors.^{29,30} However, it has been shown³⁰⁻³⁴ that a second contribution to the electron-phonon interaction, the so-called Fan^{35,36} or "self-energy" terms, is of the same order of magnitude as the Debye-Waller terms and should be included in the calculations. This has recently been done for Si and Ge³⁷⁻³⁸ as well as for GaAs,^{40,41} including the full

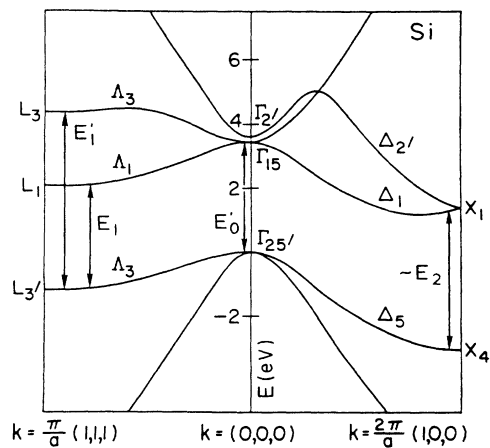


FIG. 1. Band structure of Si calculated within the $\mathbf{k}\cdot\mathbf{p}$ method (from Ref. 3), showing the main interband critical points.

band structure and phonon dispersion.

The increasing phonon-induced broadening of the CP's with rising temperature arises from the same mechanism which determines the real part of the self-energy. Results are available for Si and Ge (Ref. 42) and for GaAs.⁴¹

In this paper we investigate the temperature dependence of the optical constants and critical-point parameters of nominally undoped Si between 30 and 820 K in the photon energy range from 1.3 to 5.6 eV. We present data for the E'_0 , E_1 , E_2 , and E'_1 transitions. In Sec. II we briefly review experimental details, in Sec. III the results of the temperature dependence of the dielectric function and the analysis of the interband transitions are presented. In Sec. IV the results are discussed and compared with microscopic calculations for the energy shifts³⁹ and broadenings⁴² with temperature. Besides, the character of the E_1 transitions is comparatively discussed for several tetrahedral semiconductors. Depending on the material, these transitions can be better described by excitonic line shape or by 2D CP's.

II. EXPERIMENTAL

The measurements were performed on undoped p -type samples cut from a wafer with $p < 10^{13} \text{ cm}^{-3}$ (at room temperature) and a (111) surface orientation. The procedure of etching the sample and mounting it into the cryostat is described in Ref. 43. For the chemical treatment of the surface to be measured, a 0.05 vol % solution of Br in methanol (BrM), a 1:1 mixture $\text{NH}_4\text{OH}:\text{H}_2\text{O}$ (AmH) and a 5 vol % HF in methanol, with methanol rinsings between treatments, were used as proposed by Aspnes and Studna.⁴⁴ The details of the automatic spectral ellipsometer with rotating analyzer are described elsewhere.^{45,46} The experimental energy mesh was 10 meV, all the spectra were taken at an angle of incidence of 67.5° .

III. RESULTS

Ellipsometry measures the complex reflectance ratio ρ , defined as $\rho = r_p/r_s$, where r_p and r_s are the amplitude-

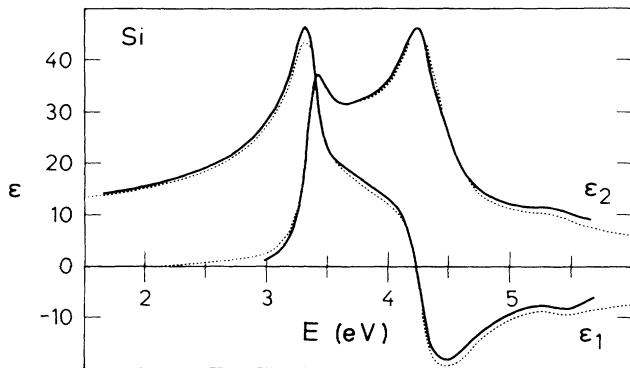


FIG. 2. Solid line: Real (ϵ_1) and imaginary (ϵ_2) part of the dielectric function of Si measured at room temperature with the sample inside a cryostat. Data are corrected for a 17.5-\AA layer of SiO_2 . Dashed line: data from Ref. 44, obtained directly after wet-chemical processing (without mounting in cryostat).

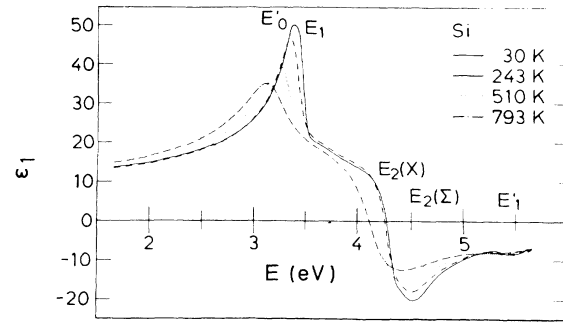


FIG. 3. Real part of the dielectric function of Si measured at several temperatures.

reflectance coefficients parallel and perpendicular to the plane of incidence, respectively. If there is no overlayer present, the dielectric function $\epsilon(\omega) = \epsilon_1(\omega) + i\epsilon_2(\omega)$ of an isotropic material is calculated within the two-phase model⁴⁷ (ambient-medium-crystal). In our case, however, due to the transfer of the sample to the cryostat and the process of outgassing, an oxide layer has grown after the chemical treatment. We therefore assume a three-phase model⁴⁷ for the sample and a dielectric function for the SiO_2 layer, taken from the literature.⁴⁸ A good agreement for the numerically calculated dielectric function of bulk-Si with the data of Ref. 44 is obtained with a layer thickness of 17.5 \AA . For comparison, we show in Fig. 2 the $\epsilon_1(\omega)$ and $\epsilon_2(\omega)$ obtained with the three-phase model with the sample mounted in the cryostat together with the data of Ref. 44 obtained directly after wet-chemical processing techniques. The agreement between both sets of data is excellent. In Figs. 3 and 4 we show the real and imaginary parts of the dielectric function of Si for several temperatures after a correction with a 17.5-\AA oxide layer with its dielectric function assumed to be temperature independent. The structures observed are attributed to E'_0 , E_1 , E_2 , and E'_1 transitions.

In order to enhance the structure in the spectra and to perform a line-shape analysis of the CP, we calculate numerically the second derivative⁴⁹ of the dielectric function with respect to photon energy $d^2\epsilon/d\omega^2$. Figure 5 shows the experimental second-derivative spectrum of ϵ_1 at 30 K in the spectral regions where structures are observed

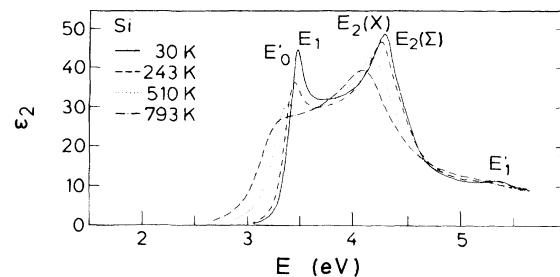


FIG. 4. Imaginary part of the dielectric function of Si measured at several temperatures.

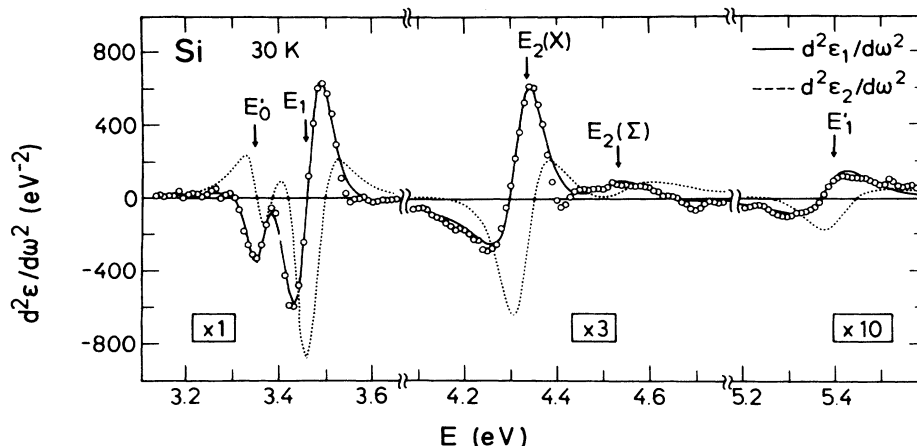


FIG. 5. Fits to the second derivatives of the real (solid line) and imaginary (dashed line) parts of the dielectric function of Si measured as a function of energy at 30 K. The readings from the vertical scale have to be divided by the factor given in the box under the various structures.

(points). The solid and dotted lines represent the best fits to standard critical-point line shapes, derived from Eq. (1):

$$\frac{d^2\epsilon}{d\omega^2} = \begin{cases} n(n-1)Ae^{i\Phi}(\omega-E+i\Gamma)^{n-2}, & n \neq 0 \\ Ae^{i\Phi}(\omega-E+i\Gamma)^{-2}, & n = 0. \end{cases} \quad (2)$$

The fit was performed simultaneously for the real and imaginary parts of $d^2\epsilon/d\omega^2$ using a least-squares procedure.

If the angle Φ in the phase factor $e^{i\Phi}$ in Eqs. (1) and (2) takes values which are integer multiples of $\pi/2$, the line shape corresponds to transitions between uncorrelated one-electron bands while noninteger multiples are usually believed to include excitonic effects by allowing a mixture of two CP integer multiple line shapes.^{1,43,50,51} In Eq. (1), taking $A > 0$ and $n = \frac{1}{2}$ for a 3D-CP, $\Phi = 0, \pi/2, \pi, 3\pi/2$ corresponds to M_1, M_2, M_3 , and M_0 CP's, respectively. By taking $A > 0$ and $n = 0$ for a 2D CP, $\Phi = 0, \pi/2, \pi$ corresponds to a minimum saddle point and maximum, respectively. For a discrete excitonic line shape ($n = -1$), a phase angle $\Phi \neq 0$ corresponds to a Fano profile, i.e., the line shape which results from the interaction of the discrete excitation with a continuous background.⁴³

The E'_0 and E_1 transitions in Si are nearly degenerate in energy and can be resolved for temperatures up to 350 K. The best fits are obtained with a 2D-CP line shape for the E'_0 CP and an excitonic line shape for the E_1 transitions. Also, this excitonic line shape yields the best fit to E_1 for the temperature above 350 K. The other structures, shown in Fig. 5, are analyzed with a 2D-CP line shape.

In Fig. 6 we show the CP energies obtained from the line-shape analysis as a function of temperature. The solid lines represent fits of the data to the empirical Varshni equation⁵²

$$E(T) = E(0) - \frac{\alpha T^2}{T + \beta}, \quad (3a)$$

or to an average Bose-Einstein statistical factor for phonons with an average frequency Θ (Refs. 42 and 46)

$$E(T) = E_B - a_B \left[1 + \frac{2}{e^{\Theta/T} - 1} \right]. \quad (3b)$$

In the 350–820-K temperature range, where the E'_0 and E_1 transitions are fitted as one structure, their temperature shift shows, within error, linear behavior:

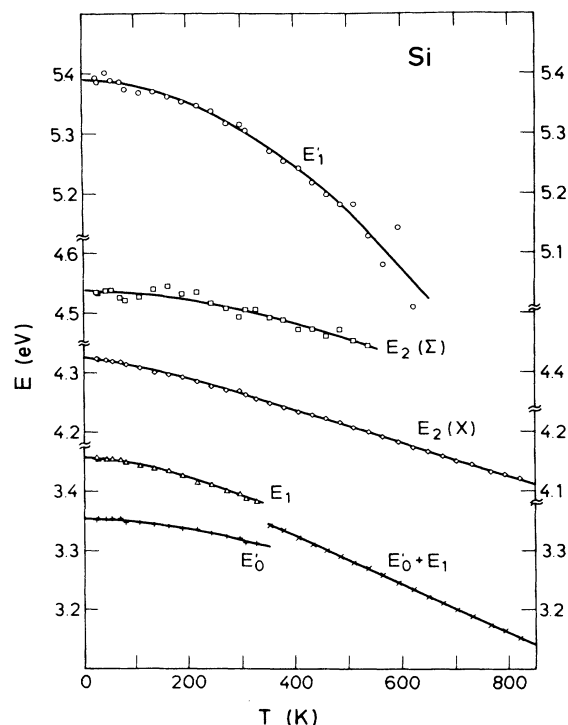


FIG. 6. Temperature dependence of the interband critical point energies of Si. The solid lines represent the best fits with Eqs. (3). The function used and the values of the parameters involved are given in Table I.

TABLE I. Parameters involved in the temperature dependence of the critical-point energies of Si. Values of the parameters $E(0)$, α , and β from the fit with $E(T) = E(0) - \alpha T^2 / (T + \beta)$, E_B , a_B , and Θ from the fit with $E(T) = E_B - a_B [1 + 2/(e^{\Theta/T} - 1)]$ and with $E(T) = E_c - \lambda T$ (for E_1 for $T > 350$ K). The 95% confidence limit is given in parentheses.

Si	$E(0)$ (eV)	α (10^{-4} eV K $^{-1}$)	β (K)	E_B (eV)	a_B (meV)	Θ (K)	Line shape
E'_0	3.354(2)	3.5(3.8)	580(970)	3.378(16)	25(17)	267(123)	2D (up to 350 K)
E_1	3.457(2)	4.7(1.7)	350(240)	3.495(13)	39(14)	245(62)	excitonic (up to 350 K)
$E_2(X)$	4.324(2)	2.87(7)	124(24)	4.349(3)	27(5)	199(30)	2D
$E_2(\Sigma)$				4.632(74)	98(76)	624(277)	2D (up to 550 K)
E'_1				5.718(176)	336(183)	703(221)	2D (up to 620 K)
Si	E_c (eV)	λ (10^{-4} eV K $^{-1}$)					Line shape
E_1	3.486(2)	4.07(3)					2D ($T > 350$ K)

$$E(T) = E_c - \lambda T. \quad (3c)$$

The values of the parameters and the equations used to describe the temperature dependence of the CP energies are listed in Table I with the corresponding uncertainties representing 95% reliability.

The temperature dependence of the broadening parameter Γ for E'_0 and E_1 are shown in the lower part of Fig. 7. Up to 350 K a formula similar to Eq. (3b) is used to describe the data:

$$\Gamma(T) = \Gamma_0 \left[1 + \frac{2}{e^{\Theta/T} - 1} \right] + \Gamma_1. \quad (4a)$$

For higher temperatures ($T > 350$) a quadratic equation

$$\Gamma(T) = \Gamma_M + cT^2 \quad (4b)$$

is used since it gives a better fit to the data. The upper part of Fig. 7 displays the temperature dependence of the broadenings of the $E_2(X)$ and E'_1 CP's where the fit was performed with Eq. (4a). The broadening of $E_2(\Sigma)$ is described by

$$\Gamma(T) = \Gamma_L + \gamma T. \quad (4c)$$

The parameters from the fit with their corresponding uncertainties are listed in Table II.

The phase angle Φ as a function of temperature is shown in Fig. 8. The label Ex means that the corresponding structure has been fitted by an excitonic line shape. Finally, the temperature dependence of amplitudes of the various transitions observed are displayed in Fig. 9.

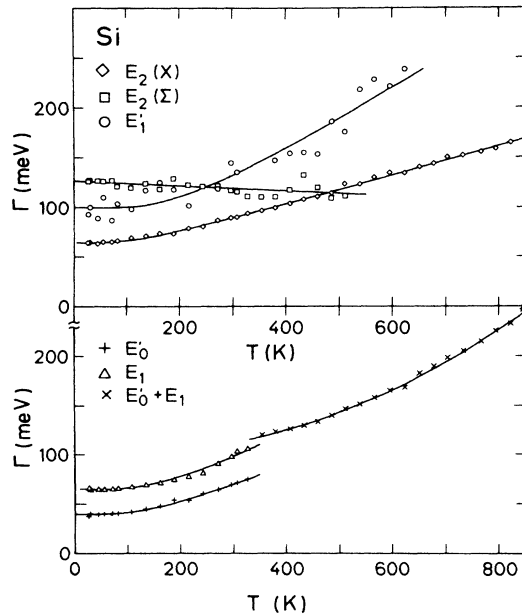


FIG. 7. Temperature dependence of the broadenings of critical points. The solid lines represent fits with Eqs. (4). The functions used and the corresponding fit parameters are given in Table II.

IV. DISCUSSION

When comparing our data for the dielectric function of Si at 300 K with those from Ref. 44 (Fig. 2), the main differences occur in the uv spectral region and in the values of ϵ_2 at energies smaller than 3.3 eV. The origin of the latter is due to the inherent poor accuracy of rotation analyzer ellipsometers for small values of ϵ_2 , as already discussed elsewhere.^{43,44} The discrepancies in the higher photon-energy region might arise from the cryostat windows:⁴³ residual piezobirefringence is expected to increase with increasing frequency.

A. $E_1 - E'_0$ transitions

The E_1 structure of Si is nearly degenerate with the E'_0 transitions. The spin-orbit splittings of the valence band are at the Γ point $\Delta_0 = 0.044$ eV,⁵³ along the Λ line $\Delta_1 \cong \frac{2}{3} \Delta_0 = 0.029$ eV,^{12,18,28} and thus cannot be resolved in the rather broad critical points observed ellipsometrically. At low temperatures the E'_0 and E_1 CP's are clearly resolved in the second-derivative spectrum $d^2\epsilon/d\omega^2$ (see Fig. 5). Up to 350 K two CP line shapes are appropriate to fit these structures. At higher temperatures only the parameters of a single critical point can be extracted from the fit to the data. The best fit is obtained by assuming an

TABLE II. Parameters involved in the temperature dependence of the broadenings of critical points in Si. Values of the parameters Γ_0 , Γ_1 and Θ , Γ_L , and γ , or Γ_M and c from the fit with $\Gamma(T)=\Gamma_0[1+2/(e^{\Theta/T}-1)]+\Gamma_1$, $\Gamma(T)=\Gamma_L+\gamma T$, or $\Gamma(T)=\Gamma_M+cT^2$. Ex means that the CP has been fitted with an excitonic line shape, 2D represents a fit with a 2D line shape. The 95% confidence limit is given in parentheses.

Si	Γ_1 (meV)	Γ_0 (meV)	Θ (K)	Γ_L (meV)	γ_B (10^{-4} eV K $^{-1}$)	Temperature range
E'_0 (2D)	0 (fixed)	39.8(9)	383(14)			30–350 K
E_1 (Ex)	0 (fixed)	65.4(1.5)	477(23)			30–350 K
$E_2(X)$ (2D)	39(3)	24(4)	326(46)			30–820 K
$E_2(\Sigma)$ (2D)				126(4)	–0.26(15)	30–550 K
E'_1 (2D)	0 (fixed)	99(8)	583(70)			30–620 K
Si	Γ_M (meV)	c (10^{-4} meV K $^{-1}$)				Temperature range
E_1 (Ex)	103(17)	2.48(52)				350–820 K

excitonic line shape for the E_1 transition, a 2D CP clearly worsens the fit. The E'_0 structure up to 350 K is best fitted with a 2D line shape (i.e., a broadened exciton and the associated interband transitions¹).

According to the theory of Toyozawa *et al.*⁵⁰ there is a coexistence of local (correlated) and band characters in the optical spectra of solids. If the band character for the electronic transition dominates, the resulting line shapes can be described by Eq. (1) with $n = -\frac{1}{2}, 0, \frac{1}{2}$. The continuous variation of Φ causes a mixture of adjacent CP's due to excitonic effects.^{1,43,50,51} In the case of a correlated excitation [$n = -1$ in Eqs. (1) and (2)] interacting with a continuum of interband transitions, the line shape is described by the Fano-Breit-Wigner profile,^{54,55} where in this case Φ is the parameter for the strength of the interaction.⁴³ For the E_1 transition of Si the localized character obviously dominates because the best fit is obtained with the excitonic line shape. For GaAs a change in the character of the transition with temperature was found, the excitonic type up to 300 K and the band character at higher temperatures,⁴³ whereas for InP, band character is kept over the 30–750-K temperature range.⁵⁶ The two limiting cases have already been observed in the thermoreflectance spectra of Ge and CdTe.⁵⁷ The dominance of correlated

transitions in CdTe is explained by higher effective mass and the lower dielectric constant [$\mu_r(\text{CdTe}) \approx 0.10$, $\epsilon(\infty) = 7.2$] in comparison with Ge [$\mu_r(\text{Ge}) \approx 0.06$, $\epsilon(\infty) = 16$]. The hydrogenic binding energy of the 2D exciton, given by¹

$$E_{\text{ex}} = \frac{2\mu_r}{[\epsilon(\infty)]^2} \quad (5)$$

is for CdTe 100 meV, about 1 order of magnitude larger than for Ge (13 meV).⁵⁷

To investigate the character of the E_1 transitions in semiconductors systematically, we have analyzed the spectra of the second derivative of the dielectric function $d^2\epsilon/d\omega^2$ for various group-IV elements and III-V and II-VI compounds. The result is shown in Table III. The

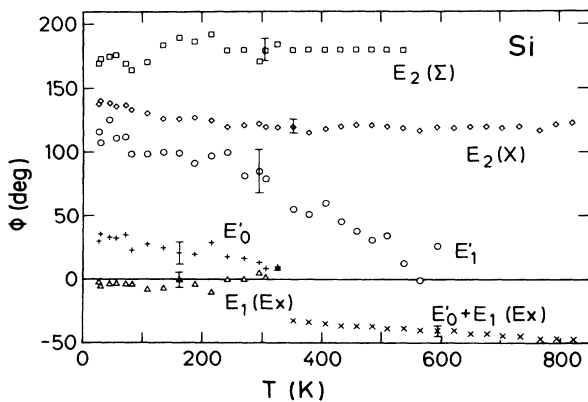


FIG. 8. Temperature dependence of the phase angle Φ , defined in Eq. (2), measured for the interband CP's of Si.

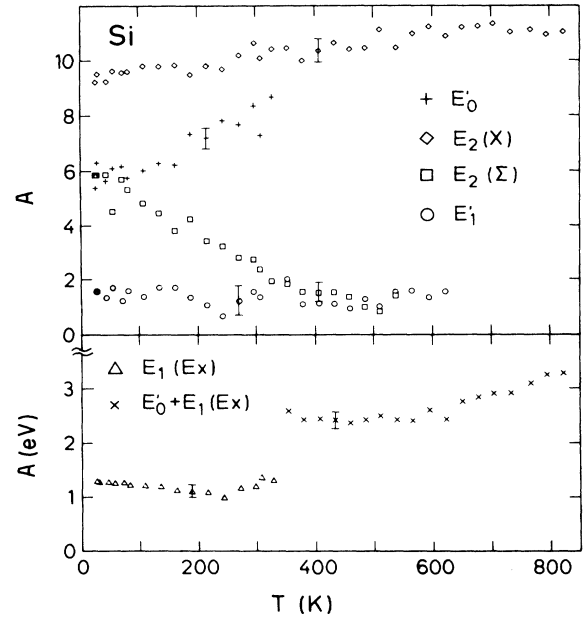


FIG. 9. Temperature dependence of the amplitudes of critical points, defined in Eq. (2), measured for Si.

TABLE III. Survey for various semiconducting materials (group-IV elements and III-V and II-VI compounds) of the character of the E_1 transition as obtained from the fit to the second derivative of the dielectric function $d^2\epsilon/d\omega^2$. For the materials in the upper right part, the localized character is dominant (better fit with an excitonic line shape), the semiconductors on the lower left show band character (better fit with a 2D line shape). The values of the high-frequency dielectric function are given in parentheses (from Ref. 58).

IV	III-V	II-VI
	Excitonic line shape	
Si (12)	AlAs	
Ge (16)	GaP (9.1)	ZnSe (5.9)
	GaAs (up to 300 K) (10.9)	
α -Sn (24)	GaAs ($T > 300$ K) (10.9)	
	GaSb (14.4)	
	InP (9.6)	CdSe (5.8)
	InSb (15.7)	CdTe (7.2)
		HgSe (7.3)
		HgTe (15.2)
2D critical point		

line shapes of the E_1 transitions of the elements or compounds in the right upper part are best fitted with an excitonic line shape, i.e., the local aspect dominates. For the materials in the lower left part a 2D CP yields the best representation of the experimental data. The values in parentheses are the high-frequency dielectric constants $\epsilon(\infty)$ taken from Ref. 58.

When going in the table from left to right the compounds show increasing ‘‘Phillips’’ ionicity f . This ionicity is $f=0$ for the group-IV elemental semiconductors, in the range $f=0.26-0.43$ for the III-V compounds, and in the range $f=0.62-0.68$ for the II-VI compound semiconductors (values for f from Ref. 59). For a given group of materials the localized-band character seems to be determined by $\epsilon(\infty)$: the higher $\epsilon(\infty)$ the lesser the localized character. This fact is easy to attribute to increased screening of the Coulomb interaction. The lowering of the dividing line from excitonic to band character with increasing ionicity f (group IV elements \rightarrow III-V compounds \rightarrow II-VI compounds) can also be attributed to the decrease in $\epsilon(\infty)$ with increasing f .

Some of our values for the energies of the E_1 transitions of Si at several temperatures are listed in Table IV and compared with other data from the literature. The shift of the critical-point energies with temperature has been calculated earlier³⁹ based on a microscopic model for the electron-phonon interaction, taking into account both Debye-Waller and self-energy terms. The total energy shift of the E'_0 and E_1 CP, obtained by adding the contributions from thermal expansion and electron-phonon interaction, is shown in Fig. 10 (solid lines), together with our experimental results. In the temperature range up to 350 K, where E'_0 and E_1 are resolved as two structures, there is excellent agreement between theory and experiment. Both calculated and experimental shifts of E'_0 with temperature are smaller than those of E_1 . At higher temperatures, where E'_0 and E_1 are fitted as one

structure, the contribution of E_1 is dominant. The temperature coefficient for this combined structure is well described by the theoretical curve for E_1 .

The dotted line is the result of ellipsometric measurements of the temperature dependence of the dielectric function by Jellison and Modine.⁷ These authors have assigned the structure in the real part of the dielectric function at 3.4 eV to E'_0 , whereas the corresponding structure in ϵ_2 was attributed to E_1 transitions, an assumption not justifiable *a priori*. In order to obtain an analytic representation of the temperature dependence of E'_0 , the Varshni equation [Eq. (3a)] was fitted by Jellison and Modine to the maxima in ϵ_1 .⁷ Their result (dotted line in Fig. 10) shows a systematic shift in energy when compared with our energies obtained from the line-shape analysis. For nonsymmetric structures neither the maximum in ϵ_1 nor that in ϵ_2 correspond to the real value of the CP energy. Only a complete line-shape analysis should thus yield reliable CP parameters.

Linear temperature coefficients over a reduced temperature range found by other authors and in the present work are given in Table V. In a recent work, Humlíček *et al.*¹⁶ have investigated the optical spectra of Si, Ge, and Si-Ge alloys. They found an average temperature shift for E_1 and E_2 interband energies from the dielectric function of -2×10^{-4} eV/K between 80 and 300 K, nearly independent of the composition of the alloy.¹⁶ The coefficient for the temperature shift of E_1 from Ref. 16 is between the coefficient for E'_0 (1.7×10^{-4} eV/K, see Table V) and E_1 (-3×10^{-4} eV/K) determined in the present work. For Ge, however, the temperature coefficient of the E_1 transitions resulting from the line-shape analysis is -4.8×10^{-4} eV/K (Ref. 46), in contrast to -2×10^{-4} eV/K from Ref. 16. The difference might be due to not having taken into account the phase angle Φ in the analysis of Ref. 16. The phase angle Φ for the E_1 transitions in Si is independent of temperature (see Fig. 8),

TABLE IV. Energies of critical points in Si at several temperatures. All values are given in eV.

Temp	E'_0	E_1	E_0 region		E_2 region		E'_1
			Experiment				
4.2 K			4.185 ^r	4.229 ^r			
5 K	3.40 ^a	3.45 ^a			4.44 ^a	4.60 ^a	5.50 ^a
10 K	3.365 ^b	3.46 ^b	4.18 ^b	4.225 ^b	4.33 ^b	4.6 ^b	5.45 ^b
					4.330 ^c		
30 K	3.355(4) ^d	3.454(2) ^d			4.323(3) ^d	4.533(11) ^d	5.387(9) ^d
80 K	3.32 ^e	3.43 ^e			4.3 ^e	4.55 ^e	
	3.34 ^f	3.42 ^f		3.88 ^f	4.26 ^f	4.46 ^f	
		3.48 ^m			4.37 ^m	4.65 ^m	
82 K	3.347(4) ^d	3.449(2) ^d			4.314(3) ^d	4.521(11) ^d	5.375(9) ^d
90 K					4.336 ^s	4.459 ^s	4.598 ^s
110 K					4.43 ^t	5.46 ^t	5.95 ^t
293 K	3.330 ^b	3.40 ^b					
296 K	3.5 ^g	3.7 ^g			4.5 ^g		
		3.38 ⁿ			4.4 ⁿ		
	3.32 ^h	3.38 ^h	4.06 ^h	4.13 ^h	4.31 ^h	4.49 ^h	
	3.281 ⁱ	3.360 ⁱ					
	3.294 ^j	3.412 ^j					
	3.34 ^k	3.41 ^k					
					4.303 ^u		
703 K	3.320(5) ^d	3.396(5) ^d			4.270(2) ^d	4.492(10) ^d	5.317(25) ^d
		3.199(4) ^d			4.150(3) ^d		
			Theory				
	3.42 ^l	3.46 ^l			4.47 ^l	4.60 ^l	5.56 ^l
		$\Delta_1=0.03^o$		$\Delta_0=0.046^o$			
		$\Delta_1=0.03^p$		$\Delta_0=0.05^p$			
		$\Delta_1=0.029^q$		$\Delta_0=0.044^q$			

^aReference 19.^bReference 12.^cReference 7.^dPresent work.^eReference 9.^fReference 20.^gReference 4.^hReference 18.ⁱReference 14.^jReference 15.^kReference 6.^lReference 25.^mReference 8.ⁿReference 5.^oReference 26.^pReference 27.^qReference 28.^rReference 11.^sReference 13.^tReference 10.^uReference 16.

whereas for Ge Φ depends strongly on temperature.⁴⁶

The phase angles Φ of the E_1 CP, analyzed with an excitonic line shape are around zero up to 350 K (see Fig. 8). Since the E_1 transitions, together with E'_0 , are the lowest direct transitions in Si, there is no continuum of band states to interact with which would cause Φ to become nonzero. For the fit of the E'_0 and E_1 CP as one structure (for $T > 350$) the mixture with the 2D minimum of E'_0 produces an apparent negative Φ . The near constancy of Φ with increasing T for most critical points studied (exception: E'_1 above 300 K) confirms the correctness of the representation chosen for those CP. The same comment can be made for the amplitude A (Fig. 9).

The temperature dependence of the broadenings Γ is caused by the electron-phonon scattering which leads to a shortening of the lifetime of electronic states and thus to an increasing broadening with increasing T . This is the same mechanism which leads to the self-energy contribution to the shift of CP energies. The corresponding temperature dependence of the CP broadening has been calculated for Si and Ge.⁴² Figure 11 shows the result for the E'_0 and E_1 transitions in comparison with the experi-

mental data reported here. The increase in the broadening with temperature is represented rather well by the theory. In order to obtain good agreement with the experimental data, however, it is necessary to add a temperature-independent contribution, which might be caused by electron-electron and surface scattering. We also note that the values of broadenings obtained from the line-shape analysis depend on the model used, e.g., the fit of a structure with the excitonic line shape [$n = -1$ in Eq. (2)] leads to a larger value than a 2D line shape [$n = 0$ in Eq. (2)]. In addition, nonparabolicities of the bands are not taken into account in the line-shape analysis; they should tend to blur the CP's and thus increase Γ .

The amplitude of the E_1 transition in Si is about 1.2 eV, nearly independent of T (see Fig. 9). The amplitude of E_1 , when treated as a 2D exciton, can theoretically be estimated by⁴³

$$A(E_1) = A_{E_1} + A_{E_1 + \Delta_1} \approx 2 \times \frac{64\sqrt{3}}{81\pi^4} \frac{a_0^3}{E^2 \epsilon_s^3} (E_1 + \Delta_1/3)^3, \quad (6)$$

TABLE V. Linear temperature coefficients of the energies of the critical points in Si. All values are given in 10^{-4} eV/K.

$-dE_{\text{ind}}/dT$	$-dE_0/dT$	$-dE'_0/dT$	$-dE_1/dT$	$-dE_2/dT$	$-dE'_1/dT$
Experiment					
Between 200 and 300 K					
2.3 ^a			2.7 ^d		
			2.2 ^e	2.2 ^e	
			2.2 ^f	2.3 ^f	
			3.6 ^g	3.5 ^g	
			2 ^h	2 ^h	
		1.7(3) ^c	3.0(2) ^c	2.5(1) ^{ij}	
				1.8(4) ^{ck}	4.5(4) ^c
Between 600 and 800 K					
			3.7 ⁱ		
			4.1(1) ^c	2.8(1) ^{ij}	
Theory					
Between 200 and 300 K					
1.7 ^b	4.7 ^b	1.5 ^b	3.3 ^b	1.9 ^l	1.5 ^b
Between 600 and 800 K					
2.4 ^b	6.2 ^b	2.4 ^b	4.3 ^b	1.8 ^b	

^aReference 52.

^bReference 39.

^cPresent work

^dReference 56.

^eReference 19.

^fReference 21.

^gReference 7.

^hReference 16.

ⁱReference 22.

^jFor $E_2(X)$.

^kFor $E_2(\Sigma)$.

^lReference 30, Penn-Model.

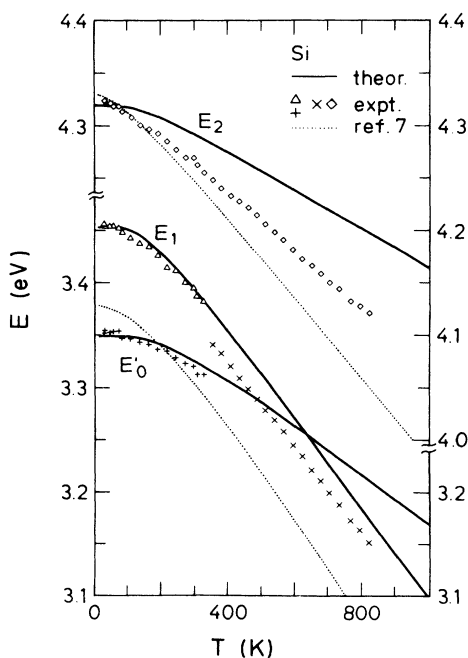


FIG. 10. Calculated and experimental shifts of critical points in Si. The solid lines show the calculated total shifts (sum of thermal expansion and contribution due to electron-phonon interaction) from Ref. 39. The dotted lines are the results from ellipsometric measurements by Jellison and Modine (Ref. 7). The points are the CP energies obtained from our line-shape analysis.

with the parameters $a_0 = 5.653 \text{ \AA}$, $E_1 = E = 3.038 \text{ eV}$, $\Delta_1 = 0$, and $\epsilon_s = 12$, for the dielectric constant we obtain $A(E_1) = 0.060 \text{ eV}$, which is a factor of 20 smaller than the experimental value of $A(E_1) = 1.2 \text{ eV}$. In Eq. (6) the amplitude is strongly dependent on the value of ϵ_s , the screening of the Coulomb potential. Screening by an effective dielectric constant $\epsilon_{\text{eff}} \approx 4.4$ would explain this discrepancy. A quantitative calculation of the space-dependent microscopic dielectric function $\tilde{\epsilon}(r)$ was per-

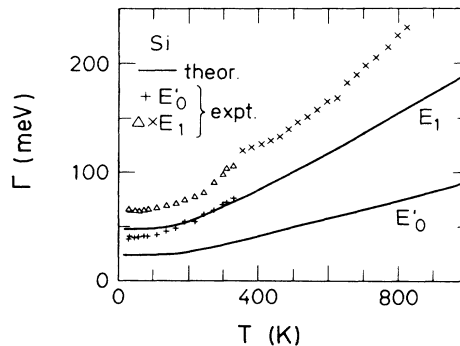


FIG. 11. Lifetime broadenings of the E'_0 and E_1 band gaps of Si. Solid line: phonon-induced broadenings, calculated in Ref. 42. Points: experimental values from this work. Up to 350 K E'_0 and E_1 have been fitted as two structures, at higher temperatures as one.

formed by Srinivasan.⁶⁰ If we assume that the “Bohr radius” of the exciton wave function is smaller than the lattice constant, a smaller value of ϵ_s should be used for the theoretical estimate of the amplitudes. According to the calculation of Ref. 60, $\epsilon_{\text{eff}}=4.4$ corresponds to a radius of 0.9 Å, somewhat less than one-half of the bond length (2.35 Å) and thus lacks physical meaning. Nevertheless, these facts seem to suggest, qualitatively, strong deviations from the Wannier-type hydrogenic behavior for the excitons related to the E_1 transitions. Similar facts were also observed for GaAs at low temperature⁴³ and, less pronounced, for InP where the band character of the E_1 transitions is dominant.⁵⁶

B. E_2 transitions

In the 4–5-eV energy range several structures have been resolved by electroreflectance at low temperatures:¹² the weak E_0 transitions at 4.18 and 4.225 eV and the E_2 transitions at 4.33 and 4.6 eV. Kondo and Moritani¹³ have pointed out that three CP can contribute to the E_2 transitions. According to the band-structure calculations of Chelikowsky and Cohen²⁵ two E_2 CP are expected at 4.47 and 4.60 eV.

The structure at 4.323 eV in Fig. 5, labeled $E_2(X)$, is attributed to transitions in a large region of \mathbf{k} space near the X point centered at $\mathbf{k}=(2\pi/a_0)(0.9,0.1,0.1)$.²⁵ The weak and broad structure at 4.544 eV, labeled $E_2(\Sigma)$, is assigned to transitions at points with Σ symmetry following Refs. 12 and 25. These transitions were resolved up to 550 K.

For both $E_2(X)$ and $E_2(\Sigma)$ a 2D line shape yields the best representation of the data. The parameters from the line-shape analysis as a function of temperature are shown in Figs. 6–9, a comparison of the CP energies with data from the literature is performed in Table IV. The phase angles Φ are nearly independent of temperature. Also, the amplitude of $E_2(X)$ is almost constant, whereas the one for $E_2(\Sigma)$ decreases with temperature.

The comparison of the temperature shift of the $E_2(X)$ gap with the theoretical results of Ref. 39 is shown in Fig. 10. The dotted line represents the experimental results of Jellison and Modine⁷ obtained from the shift of the maximum of the imaginary part of the dielectric function with temperature: the results from our line-shape analysis show a smaller temperature shift in better agreement with the calculations. The remaining discrepancy of experimental and theoretical results might be due to the uncertainty in the location of the E_2 transitions in \mathbf{k} space and to the fact that the band structure used for the calculations in Ref. 39 underestimates the E_2 CP energies by about 10%. Besides, the calculations were performed only for one representative \mathbf{k} point, namely $\mathbf{k}=2\pi/a_0(0.9,0.1,0.1)$.³⁹

The comparison of the experimental results for the lifetime broadening of the $E_2(X)$ CP and theoretical ones⁴² is given in Fig. 12. The calculations have been performed for the same representative point as for the energy shifts.

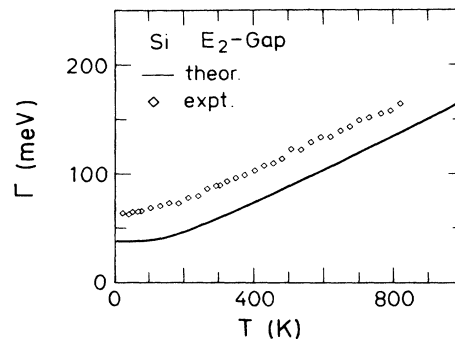


FIG. 12. Lifetime broadenings of the E_2 band gap of Si. Solid line: phonon-induced broadening, calculated in Ref. 42 for the representative point $\mathbf{k}=(2\pi/a_0)(0.9,0.1,0.1)$. Points: experimental values for $E_2(X)$ from this work.

Like the case of the E_1 and E'_0 transitions, the addition of a constant broadening of about 30 meV for the E_2 CP yields excellent agreement between theory and experiment.

C. E'_1 transitions

The E'_1 transitions take place between the Λ_3 valence band and the Λ_3 conduction band (see Fig. 1). At low temperatures the energy of 5.45 eV was measured by electroreflectance.¹² In Fig. 5 the weak structure at 5.387 eV (30 K) is attributed to the E'_1 CP. A line-shape analysis of this structure with a 2D CP was possible up to 600 K. The corresponding CP parameters are shown in Figs. 6–9 as a function of temperature.

V. CONCLUSION

The temperature dependence of the dielectric function was measured in the 1.7–5.7-eV energy range up to 820 K. By performing a line-shape analysis of the structures observed, the parameters of the E'_0 , E_1 , E_2 , and E'_1 critical points (amplitude, threshold energy, lifetime broadening, phase angle) were obtained as a function of temperature. Comparison with earlier calculations of the energy shift and broadenings based on the electron-phonon interaction shows, in most cases, excellent agreement between theory and experiment. A careful analysis of the E_1 transitions of Si and other semiconductors shows a systematic change in the character of these transitions from a localized Lorentzian interacting with the continuum to a two-dimensional Van Hove singularity modified by the electron-hole interaction both with increasing ionicity and increasing average atomic number.

ACKNOWLEDGMENTS

One of us (M.G.) acknowledges financial support of Caixa de Pensions “la Caixa” (Barcelona, Spain). We would like to thank M. Bleder and A. Birkner for help with the construction of the ellipsometer and H. Hirt, M. Siemers, and P. Wurster for expert technical help.

- *Present address: Instituto de Ciencia de Materiales del Consejo Superior de Investigaciones Científicas, Universidad de Zaragoza, E-50009 Zaragoza, Spain.
- ¹M. Cardona, *Modulation Spectroscopy*, Suppl. 11 of *Solid State Physics*, edited by F. Seitz, D. Turnbull, and H. Ehrenreich (Academic, New York, 1969).
 - ²D. E. Aspnes, in *Handbook on Semiconductors*, edited by M. Balkanski (North-Holland, Amsterdam, 1980), Vol. 2, p. 109.
 - ³C. W. Higginbotham, Ph.D. thesis, Brown University, 1967 (unpublished); M. Cardona and F. H. Pollak, *Phys. Rev.* **142**, 530 (1966).
 - ⁴H. Ehrenreich, H. R. Philipp, and J. C. Phillips, *Phys. Rev. Lett.* **8**, 59 (1962).
 - ⁵M. Cardona and D. L. Greenaway, *Phys. Rev.* **125**, 1291 (1962).
 - ⁶G. Jungk, *Phys. Status Solidi B* **99**, 643 (1980).
 - ⁷G. E. Jellison, Jr., and F. A. Modine, *Phys. Rev. B* **27**, 7466 (1983).
 - ⁸S. O. Sari and S. E. Schnatterly, *Surf. Sci.* **37**, 328 (1973).
 - ⁹E. Matatagui, A. G. Thompson, and M. Cardona, *Phys. Rev.* **176**, 950 (1968).
 - ¹⁰G. Guizzetti, L. Nosenzo, E. Reguzzoni, and G. Samoggia, *Phys. Rev. B* **9**, 640 (1974).
 - ¹¹D. E. Aspnes and A. A. Studna, *Solid State Commun.* **11**, 1375 (1972).
 - ¹²A. Daunois and D. E. Aspnes, *Phys. Rev. B* **18**, 1824 (1978).
 - ¹³K. Kondo and A. Moritani, *Phys. Rev. B* **15**, 812 (1977).
 - ¹⁴J. W. Grover and P. Handler, *Phys. Rev. B* **9**, 2600 (1974).
 - ¹⁵K. Kondo and A. Moritani, *Phys. Rev. B* **14**, 1577 (1976).
 - ¹⁶J. Humlíček, F. Lukeš, E. Schmidt, M. G. Kekoua, and E. Khoutsishvilli, *Solid State Commun.* **47**, 387 (1983).
 - ¹⁷J. S. Kline, F. H. Pollak, and M. Cardona, *Helv. Phys. Acta.* **41**, 968 (1968).
 - ¹⁸M. Cardona, K. L. Shaklee, and F. H. Pollak, *Phys. Rev.* **154**, 696 (1967).
 - ¹⁹R. R. L. Zucca and Y. R. Shen, *Phys. Rev. B* **1**, 2668 (1970).
 - ²⁰M. Welkowsky and R. Braunstein, *Phys. Rev. B* **5**, 497 (1972).
 - ²¹D. Auvergne, J. Camassel, H. Mathieu, and M. Cardona, *Phys. Rev. B* **9**, 5168 (1974).
 - ²²A. Compaan and H. J. Trodahl, *Phys. Rev. B* **29**, 793 (1984).
 - ²³M. L. Cohen and T. K. Bergstresser, *Phys. Rev.* **141**, 789 (1966).
 - ²⁴M. Cardona and F. H. Pollak, *Phys. Rev. B* **142**, 530 (1966).
 - ²⁵J. R. Chelikowsky and M. L. Cohen, *Phys. Rev. B* **14**, 556 (1976).
 - ²⁶F. Herman, R. L. Kortum, C. D. Kuglin, J. P. Van Dyke, and S. Skillman, in *Methods in Computational Physics*, edited by B. Adler, S. Fernbach, and M. Rotenberg (Academic, New York, 1968), Vol. 8, p. 193.
 - ²⁷G. S. Wepfer, T. C. Collins, and R. N. Euwema, *Phys. Rev. B* **4**, 1296 (1971).
 - ²⁸D. J. Chadi, *Phys. Rev. B* **16**, 790 (1977).
 - ²⁹E. Antončík, *Czech. J. Phys.* **5**, 449 (1955).
 - ³⁰P. Y. Yu and M. Cardona, *Phys. Rev. B* **2**, 3193 (1970).
 - ³¹P. B. Allen and V. Heine, *J. Phys. C* **9**, 2305 (1976).
 - ³²M. Schlüter, G. Martinez, and M. L. Cohen, *Phys. Rev. B* **12**, 650 (1975).
 - ³³P. B. Allen, *Phys. Rev. B* **18**, 5217 (1978).
 - ³⁴B. Chakraborty and P. B. Allen, *J. Phys. C* **11**, L9 (1978); *Phys. Rev. B* **18**, 5225 (1978).
 - ³⁵H. Y. Fan, *Phys. Rev.* **82**, 900 (1951).
 - ³⁶M. L. Cohen, *Phys. Rev.* **128**, 131 (1962).
 - ³⁷P. B. Allen and M. Cardona, *Phys. Rev. B* **23**, 1495 (1981); **24**, 7479 (1981).
 - ³⁸P. B. Allen and M. Cardona, *Phys. Rev. B* **27**, 4760 (1983).
 - ³⁹P. Lautenschlager, P. B. Allen, and M. Cardona, *Phys. Rev. B* **31**, 2163 (1985).
 - ⁴⁰C. K. Kim, P. Lautenschlager, and M. Cardona, *Solid State Commun.* **59**, 797 (1986).
 - ⁴¹S. Gopalan, P. Lautenschlager, and M. Cardona, *Phys. Rev. B* **35**, 5577 (1987).
 - ⁴²P. Lautenschlager, P. B. Allen, and M. Cardona, *Phys. Rev. B* **33**, 5501 (1986).
 - ⁴³P. Lautenschlager, M. Garriga, S. Logothetidis, and M. Cardona, *Phys. Rev. B* **35**, 9174 (1987).
 - ⁴⁴D. E. Aspnes and A. A. Studna, *Phys. Rev. B* **27**, 985 (1983).
 - ⁴⁵D. E. Aspnes, *Opt. Commun.* **8**, 222 (1973); D. E. Aspnes and A. A. Studna, *Appl. Opt.* **14**, 220 (1975); *Rev. Sci. Instrum.* **49**, 291 (1978).
 - ⁴⁶L. Viña, S. Logothetidis, and M. Cardona, *Phys. Rev. B* **30**, 1979 (1984).
 - ⁴⁷R. M. Azzam and N. M. Bashara, *Ellipsometry and Polarized Light* (North-Holland, Amsterdam, 1977).
 - ⁴⁸*American Institute of Physics Handbook*, 3rd ed, edited by D. E. Gray (McGraw-Hill, New York, 1972).
 - ⁴⁹A. Savitzky and M. J. E. Golay, *Anal. Chem.* **36**, 1627 (1964); J. Steinier, Y. Termonia, and J. Deltour, **44**, 1906(E) (1972).
 - ⁵⁰Y. Toyozawa, M. Inoue, T. Inui, M. Okazaki, and E. Hanamura, *J. Phys. Soc. Jpn. Suppl.* **21**, 133 (1966); *J. Phys. Soc. Jpn.*, **22**, 1337 (1967).
 - ⁵¹J. E. Rowe and D. E. Aspnes, *Phys. Rev. Lett.* **25**, 162 (1970).
 - ⁵²Y. P. Varshni, *Physica (Utrecht)* **34**, 149 (1967).
 - ⁵³S. Zwerdling, K. J. Button, B. Lax, and L. M. Roth, *Phys. Rev. Lett.* **4**, 173 (1960).
 - ⁵⁴U. Fano, *Phys. Rev.* **124**, 1866 (1961).
 - ⁵⁵G. Abstreiter, M. Cardona, and A. Pinczuk, in *Light Scattering in Solids IV*, edited by M. Cardona and G. Güntherodt (Springer-Verlag, Berlin, 1984), p. 5.
 - ⁵⁶P. Lautenschlager, M. Garriga, and M. Cardona, *Phys. Rev. B* **36**, 4813 (1986).
 - ⁵⁷S. Antoci, E. Reguzzoni, and G. Samoggia, *Solid State Commun.* **9**, 1081 (1971).
 - ⁵⁸Landolt-Börnstein, in *Semiconductors*, edited by O. Madelung, M. Schulz, and H. Weiss (Springer, Berlin, 1982), Vols. 17a and 17b.
 - ⁵⁹J. C. Phillips, in *Handbook on Semiconductors*, edited by W. Paul (North-Holland, Amsterdam, 1982), Vol. 1, Ch. 4C.
 - ⁶⁰G. Srinivasan, *Phys. Rev.* **178**, 1244 (1969).